A DNA aptamer recognizing MMP14 for *in vivo* and *in vitro* imaging identified by cell-SELEX

XUFANG HUANG*, JINMAN ZHONG*, JING REN, DIDI WEN, WEIWEI ZHAO and YI HUAN

Department of Radiology, Xijing Hospital, Fourth Military Medical University, Xi'an, Shaanxi 710032, P.R. China

Received March 22, 2018; Accepted April 17, 2019

DOI: 10.3892/ol.2019.10282

Abstract. A key challenge for the management of various types of cancer, including pancreatic cancer and hepatocellular carcinoma, is accurate diagnosis at an early stage. Matrix metalloproteinase 14 (MMP14) is overexpressed in numerous types of cancer and is associated with poor prognosis. Therefore, MMP14-specific imaging probes have potential use in the diagnosis of MMP14-positive cancer. Aptamers are short oligonucleotide sequences that can bind to molecular targets with a high specificity and affinity. Aptamers are typically obtained from an *in vitro* library; this process is usually termed systematic evolution of ligands by exponential enrichment (SELEX). In the present study, a DNA aptamer targeting MMP14 was obtained by cell-SELEX and termed M17, which specifically recognizes MMP14-positive cells. Aptamer M17 selectively binds to membrane proteins of MMP14-transfected 293T cells (Kd, 4.98±1.26 nM). Pancreatic cancer cell imaging suggested that aptamer M17 can bind to the cell membranes of two pancreatic cancer cell lines (MIA PaCa-2 and PANC-1). *In vivo* tumor imaging demonstrated that the targeting recognition of MIA PaCa-2 tumor cells in mice could be visualized using Cy5-labeled aptamer M17. Aptamer M17-conjugated polyethylene glycol-Fe3O4 can specifically bind to MIA PaCa-2 and PANC-1 cells, and reduce MRI T2-weighted imaging signal intensity. The DNA aptamer M17 has the advantages of simplicity of synthesis, small size, low immunogenicity, high penetrability and high affinity. Therefore, aptamer M17 is a potential molecular probe for the diagnosis and treatment of MMP14-positive cancer.

Correspondence to: Professor Yi Huan, Department of Radiology, Xijing Hospital, Fourth Military Medical University, 127 Changle West Road, Xi'an, Shaanxi 710032, P.R. China
E-mail: yihuan0007@163.com

*Contributed equally

Key words: DNA aptamer, matrix metalloproteinase 14, magnetic resonance imaging, cell-systematic evolution of ligands by exponential enrichment, pancreatic cancer

Introduction

The matrix metalloproteinase (MMP) family is a group of zinc-binding endopeptidases that are involved in the breakdown of extracellular matrix (1). The majority of MMPs are secreted proteins that are activated by extracellular proteinases. The membrane-type MMP (MT-MMP) subfamily is a subtype of MMPs, which contain transmembrane domains and are expressed on the surface of the cell membrane. MMP14 (also termed MT1-MMP) is a member of this subfamily, containing a C-terminal hydrophobic stretch to anchor the protein to the cell membrane surface and to exert its effect. MMP14 activates MMP2, which is closely associated with the invasion and metastasis of cancer (2,3). MMP14 has also been demonstrated to be associated with angiogenesis and cell migration (4,5). Wickramasinghe *et al* (6) reported the isolation of a peptide aptamer termed swiggle that interacts with the intracellular domain of MMP14 and swiggle-mediated inhibition of clathrin-mediated MMP14 internalisation was identified to promote MMP14-mediated cell migration. MMP14 is overexpressed in numerous types of cancer and is associated with a poor prognosis of pancreatic cancer (7,8), hepatocellular carcinoma (9), lung carcinomas (10-13), gastrointestinal carcinomas (14-17), breast carcinomas (12,18,19), gliomas (20) and cervical carcinomas (21). We previously analyzed the expression of MMP14 in pancreatic cancer tissues and surrounding normal pancreatic tissues, which revealed that MMP14 was highly expressed in the pancreatic cancer group, while the surrounding pancreatic tissue had a low expression level (22). Therefore, MMP14 has great application prospects as a tumor biomarker (23). Previously, there have been a number of reports of MMP14-specific functional blocking antibodies (4,24-27) and nanosensors (28), which indicate MMP14 may be a useful tool for diagnostic and therapeutic applications.

Aptamers can bind to target molecules with high specificity via their specific three-dimensional structures; therefore, aptamers are chemical antibodies (29). More specifically, nucleic acid aptamers include short DNA and RNA aptamers. Cell-systematic evolution of ligands by exponential enrichment (SELEX) is an improvement of the conventional SELEX, which uses live cells as the screening object to obtain aptamers of target molecules in the natural state of the cell surface (29-32). In order to reduce non-specific aptamers, negative screening cells are usually introduced (29). Compared

with antibodies, aptamers have the advantages of cost, easy synthesis, controllable modification, low toxicity, low immunogenicity, long-term stability and a small size (33). Based on these advantages, aptamers have become a popular topic in molecular imaging and targeted therapy (34-40). For example, by modifying the superparamagnetic iron oxide nanoparticle (SPION) and doxorubicin co-loaded polymer with aptamer AS1411 as a targeting agent, the probe could be used not only for magnetic resonance imaging (MRI) of colon carcinoma xenografts, but also as a tumor-targeted delivery system (36). Therefore, aptamers exhibit great application prospects in molecular imaging and targeted therapy of tumors as targeted tracers.

In the present study, 293T cells transfected with the recombinant MMP14 gene were used as target cells to obtain the DNA aptamer M17, which specifically recognizes MMP14-positive cells through cell-SELEX technology, and its application potential in imaging was further investigated. Aptamer M17 could be used to target pancreatic cancer xenografts in fluorescent imaging. In addition, M17 aptamer was conjugated to the surface of SPIONs through a biotin-streptavidin system and the probe could effectively reduce the T2-weighted MRI signal intensity of two pancreatic cancer cell lines *in vitro*.

Materials and methods

Cell lines and cell culture. The 293T, PANC-1, MIA PaCa-2, HepG2 and MCF-7 cell lines were provided by the Department of Biochemistry and Molecular Biology, The Air Force Medical University (Xi'an, China). All cell lines were grown in Dulbecco's modified Eagle's medium (Thermo Fisher Scientific, Inc., Waltham, MA, USA) containing 10% fetal bovine serum (Thermo Fisher Scientific, Inc.) and incubated in 5% CO_2 at 37˚C.

Construction of recombinant vector and transfection. MMP14 complementary DNA was synthesized and spliced into CD510B-1 plasmids (System Biosciences, LLC., Palo Alto, California, USA). The sequence of the synthetic plasmid, CD510B-1-MMP14, was confirmed through DNA sequencing by Sangon Biotech Co., Ltd. (Shanghai, China). A total of 5 μg CD510B-1-MMP14 plasmids were transfected into 293T cells in a 60-mm dish using 15 μl TransEasy transfection reagent (Foregene, Shanghai, China). Untreated CD510B-1 plasmids were transfected into 293T cells using the same method and served as a control group termed 293T-Plasmid cells. Following 36 h of transfection, the expression of MMP14 in the transfected cells was confirmed by western blotting using an anti-MMP14 antibody (Abcam, Cambridge, UK).

SELEX single-stranded DNA (ssDNA) library and primers. The random sequence library and primers were synthesized and purified by Sangon Biotech Co., Ltd. The random sequence library consisted of three parts; the random part, composed of 40 randomized nucleotides located in the center of the sequence, and two constant parts, composed of 20 nucleotides respectively located at both ends of the sequence. The sequence was as follows: 5'-TGCGGAAGCCACCAG GAGTT(40N)ACGAGCCAAAGAGCCGCCAA-3', where 40N indicates the 40 randomized nucleotides. The forward primer sequence was 5'-TGCGGAAGCCACCAGGAGT-3' and its 5' end was labeled with 5-carboxyfluorescein (FAM). The reverse primer sequence was 5'-TTGGCGGCTCTTTGG CTCGT-3', which was labeled with biotin at the 5' end.

Cell-SELEX. The initial random sequence library of 5 nM was dissolved in 200 μl binding buffer (Genshare Biological, Xi'an, China) and then denatured for 5 min at 95˚C, followed by immediate cooling for 10 min on ice. Prior to screening, the 293T-MMP14 cells were gently washed twice with PBS for 3 min. The cells (~$0.5x10^5/cm^2$) were incubated for 2 h with the library at 37˚C. To remove the unbound sequences, following incubation the cells were gently washed three times for 3 min washing buffer (Genshare Biological). The cells were collected and kept in a 95˚C water bath for 5 min and then immediately cooled for 10 min on ice. The cell-bound ssDNAs were extracted using phenol, chloroform and isopropanol. The cell-bound ssDNA was precipitated by sodium acetate and pre-cooled with isopropanol for 3 h at -20˚C. The sediment was dissolved in 200 μl ultrapure water. This solution was then amplified by polymerase chain reaction (PCR) using Taq polymerase and dNTPs from Takara Biotechnology Co., Ltd. (Dalian, China). The PCR conditions were as follows: 95˚C for 5 min, followed by 30 cycles of 95˚C for 10 sec, 57˚C for 10 sec, 72˚C for 10 sec and 72˚C for 5 min. The PCR product was co-incubated with streptavidin-labeled magnetic beads (BeaverBeads, Suzhou, China) and the double-stranded DNA sequences were bound to the magnetic beads via biotin-streptavidin. Following denaturation in 0.15 M NaOH, the positive strand of DNA was dissociated, collected and used for the next round of screening. The first round of screening using the library labeled with FAM was obtained via asymmetric PCR as aforementioned, except that the forward primers were labeled with FAM, and flow cytometry, performed as aforementioned, was used to monitor the effect of screening. From the third to the twelfth round, the next-round library was incubated with the cells of the control group and the unbound sequences were collected and incubated with the target cells. In order to obtain high-specificity and high-affinity aptamers, with increasing rounds of screening, the incubation time with the target cells was gradually decreased from 120 to 30 min, while the time with the cells of the control group was gradually increased from 30 min to 2 h. The washing time following incubation with the target cells was gradually increased. After 12 rounds of screening, the screened ssDNA library was cloned into the plasmid using a M5 HiPer pTOPO-Blunt Cloning kit (Mei5 Biotechnology, Co., Ltd, Beijing, China). Subsequently, the products were transformed into DH5α competent cell-coated plates for monoclonal colony selection and sequencing by Sangon Biotech Co., Ltd. The secondary structure of the finally obtained aptamers were predicted using the RNA structure. To do so, first open the URL (http://rna.urmc.rochester.edu/RNAstructureWeb/), then enter the aptamer name and sequence, select the nucleic acid type as DNA, and finally click the 'submit query' to obtain the predicted secondary structure of the aptamers.

Flow cytometry. After cells were detached by treatment with 0.1% trypsin-0.02% EDTA solution, cells were placed in fetal calf serum (FCS)-supplemented medium to inactivate

Table I. Percentage of fluorescent-labeled cells for cell-systematic evolution of ligands by exponential enrichment.

	Ratio of positive cells, %	
	293T-MMP14	293T-Plasmid
Cell	0.16	1.38
Lib	3.65	4.80
3th	19.5	6.24
6th	48.7	8.66
9th	84.5	1.57
12th	95.3	1.38

Lib, initial library; MMP14, matrix metalloproteinase 14; Cell, blank control.

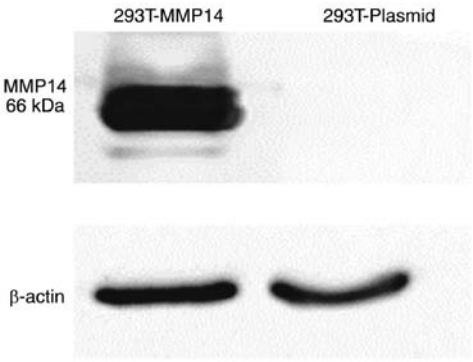

Figure 1. Expression of MMP14 protein in 293T-MMP14 cells was analyzed by western blotting. β-actin was used as an internal control. MMP14, matrix metalloproteinase 14.

trypsin and EDTA. Then the cells were treated with labeling solution (Genshare Biological) at 37˚C for 30 min. In total, ~2x10^5 cells were incubated for 30 min at 37˚C in the dark with the FAM-labeled random sequence library or next round library (20 nM) or aptamers (2 nM) in PBS binding buffer (200 μl) containing 10% FCS and 0.02% NaN3. After incubation, the cells were washed thrice using 1,000 μl PBS washing buffer containing 10% FCS, then re-suspended in 200 μl binding buffer. The incubated cells were analyzed for FAM using a flow cytometer. FlowJo7.0 software (version 7.0; FlowJo LLC, Ashland, OR, USA) was used for the analysis of the flow cytometry data. The dissociation constant (Kd) of the aptamer and target cells was quantified using the one-site saturation equation: Y=Bmax x X/(Kd + X), where Y is fluorescence intensity of the cells and X is concentration of the aptamer and Bmax is maximum binding potential. Analysis was performed used Sigma Plot 12.5 software (http://www.sigmaplot.co.uk/products/sigmaplot/sigmaplot-details.php).

Laser scanning confocal microscopy (LSCM). In total, ~1x10^5 293T-MMP14 cells or 293T-Plasmid cells were seeded in 35-mm dishes for LSCM. When the cells reached 80% confluency, the cell culture medium was discarded. Following three gentle washes with PBS, the cells were fixed for 15 min with 4% paraformaldehyde at room temperature, and then blocked for 30 min with 1% bovine serum albumin at room temperature. The cells were then incubated for 30 min with 20 nM FAM-labeled aptamers at 37˚C and the cell nucleus was stained with DAPI for 5 min at room temperature. The cells were finally imaged by LSCM (magnification, x800). Pancreatic cancer cells were seeded and cultured in the same way. Following washing with PBS, the target cells were incubated for 30 min with 20 nM Cy5-labeled aptamers at 37˚C and then images were obtained by LSCM (magnification x400).

Western blot analysis. The western blot analysis was performed in accordance with the protocol by Abcam. Proteins were extracted using 10x RIPA Buffer (Abcam) and determined using the BCA method. Proteins were loaded onto a polyacrylamide gel (10% gel) at a mass of 20 μg per lane, and separated via constant pressure electrophoresis. The concentration of the gel was 10%. The protein in the gel was transferred under constant voltage to a polyvinylidene difluoride (PVDF) membrane. Following blocking for 1 h at room temperature with PBS containing 5% skimed milk, the PVDF membrane was incubated with anti-MMP14 antibody (1:5,000; ab51074; Abcam) at 4˚C overnight. After washing three times with TBS containing 0.1% tween, the membrane was incubated with the secondary antibody labeled with horseradish peroxidase (HRP; 1:10,000; ab6721; Abcam) for 1 h at room temperature. Finally, the immunoreactive bands were visualized by a Chemiluminescent HRP Substrate (Abcam).

In vivo fluorescence imaging. A total of 30 Athymic BALB/c, 4-week-old mice (15 male, 15 female) were provided by the Experimental Animal Center of the Air Force Medical University (Xi'an, China). The average weight of the males was 17 g, and the average weight of the females was 14 g. The housing criteria of the mice was set up as per guidelines from the Experimental Animal Center of the Air Force Medical University. The tumor-bearing nude mouse model was generated by subcutaneously injecting 1x10^7 MIA PaCa-2 cells in suspension into the axilla of the mice. Tumors were observed until they reached 1.0 cm in diameter. The mice were anesthetized using a small animal anesthesia system (E-Z Anesthesia EZ-7000 classic system, E-Z Anesthesia, Palmer, PA, USA). The animal study was approved by the Ethics Committee of the Experimental Animal Center of the Air Force Medical University. When the mice were anesthetized, 100 nM Cy5-labeled aptamer M17 or the initial library was injected through the tail vein. At different time points, the Cy5 fluorescence signal of the mice was acquired by a whole body imaging system (IVIS Lumina II Series, Caliper Life Sciences; PerkinElmer, Inc., Waltham, MA, USA).

Synthesis of aptamer-conjugated magnetic nanoparticles and in vitro MRI. Streptavidin-coated polyethylene glycol (PEG)-Fe3O4 nanoparticles (Nanjing Nanoeast Biological Technology Co., Ltd., Nanjing, China) were reacted with biotin-labeled M17 and the unselected initial library separately for 1 h on a shaker to generate the M17-SPIONs and Lib-SPIONs, respectively, through a biotin-streptavidin

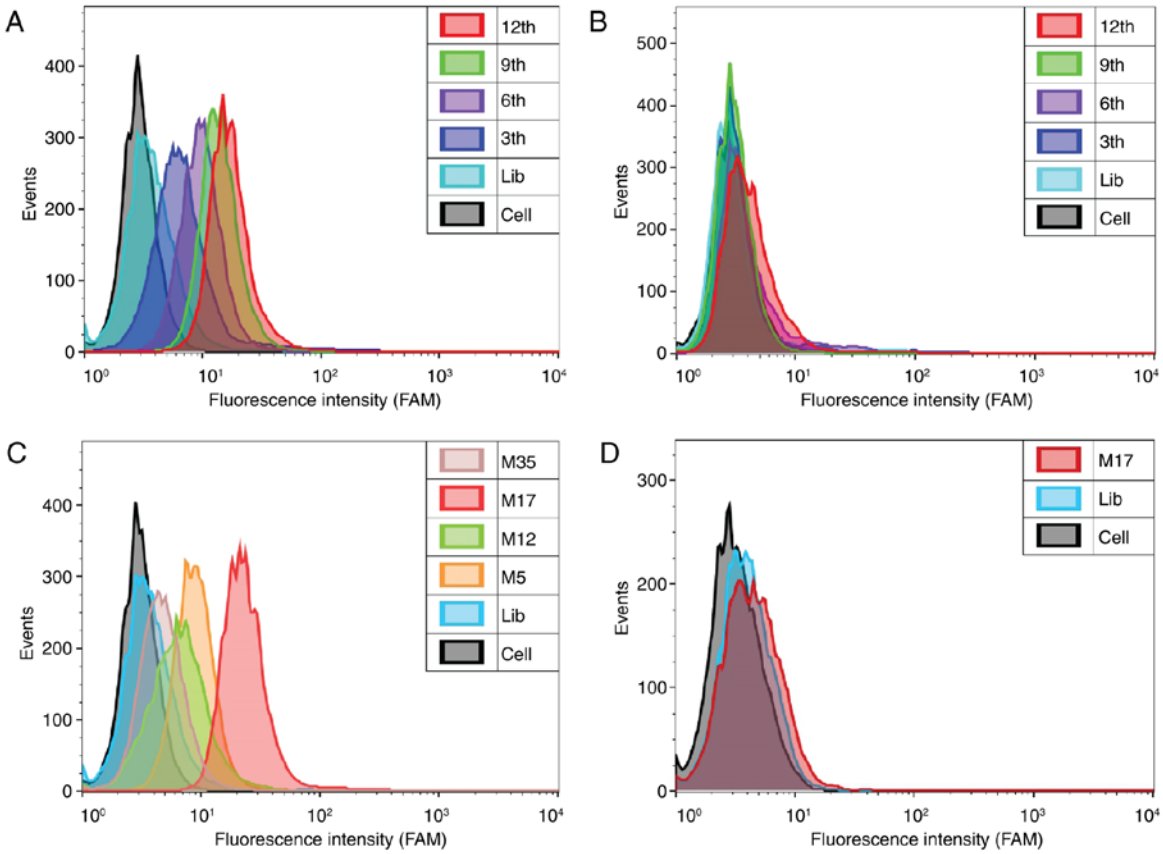

Figure 2. Flow cytometry measurements. Flow cytometry was used to monitor the binding ability of the selected libraries with (A) 293T-MMP14 cells and (B) 293T-Plasmid cells, and the FAM-labeled aptamer candidates to (C) 293T-MMP14 cells and (D) control cells. Lib was used as a negative control. MMP14, matrix metalloproteinase 14; FAM, 5-carboxyfluorescein; Lib, initial library; Cell, blank control.

system. The probes were gathered by magnetic separation and finally re-suspended in 3% agarose gel to the required concentration. The relaxivity of the magnetic nanoparticles was measured using a Siemens 3.0T MRI scanner (Siemens AG, Munich, Germany) when the solution was solidified. The T2 weighted imaging (T2WI) measurement parameters were as follows: Time of repetition, 3,500 ms; time of echo, 91 ms; averages, 8; and field of field, 100 mm. TR is time of repetition, TE is time of echo, FOV is field of view. Subsequently, ~1x10^7 target cells were incubated with M17-SPIONs and Lib-SPIONs at 37˚C for 1 h. Then the cells were washed thrice with PBS and resuspended in 3% agarose gel and scanned with an MRI scanner when the solution was solidified. 293T cells were used as a negative control.

Statistical analysis. All measurement data is presented as the mean ± standard deviation. The data were analyzed using a two-sample Student's t-test and Pearson's correlation analysis using SPSS software (version 17.0; SPSS, Inc., Chicago, IL, USA). $P<0.05$ was considered to indicate a statistically significant difference.

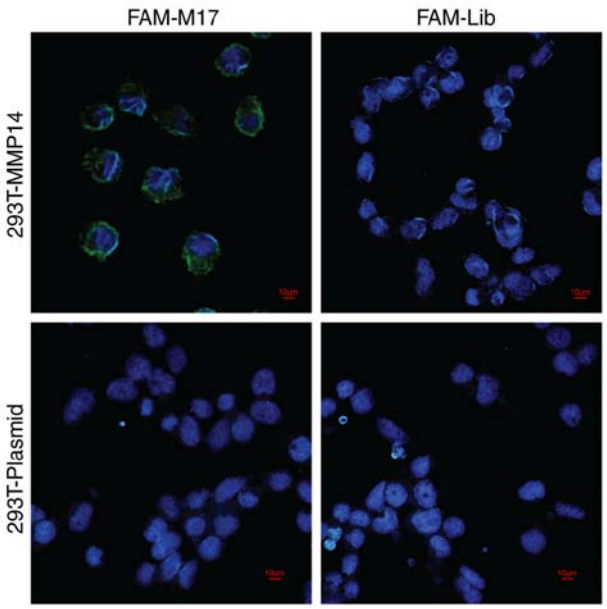

Figure 3. Binding specificity assays of the FAM-M17 to 293T-MMP14 cells and 293T-Plasmid cells by laser scanning confocal microscopy. Lib was used as a control. Scale bar, 10 μm. MMP14, matrix metalloproteinase 14; FAM, 5-carboxyfluorescein; Lib, initial library.

Results and Discussion

Expression of MMP14 in transfected cells. To effectively screen aptamers that specifically recognize MMP14, MMP14 was overexpressed in 293T cells while maintaining its native conformation on the cell membrane. The cells of the negative control group expressed a low level of MMP14. 293T-MMP14 cells and 293T-Plasmid cells were obtained by transfecting CD510B-1-MMP14 and CD510B-1 plasmids, respectively, into

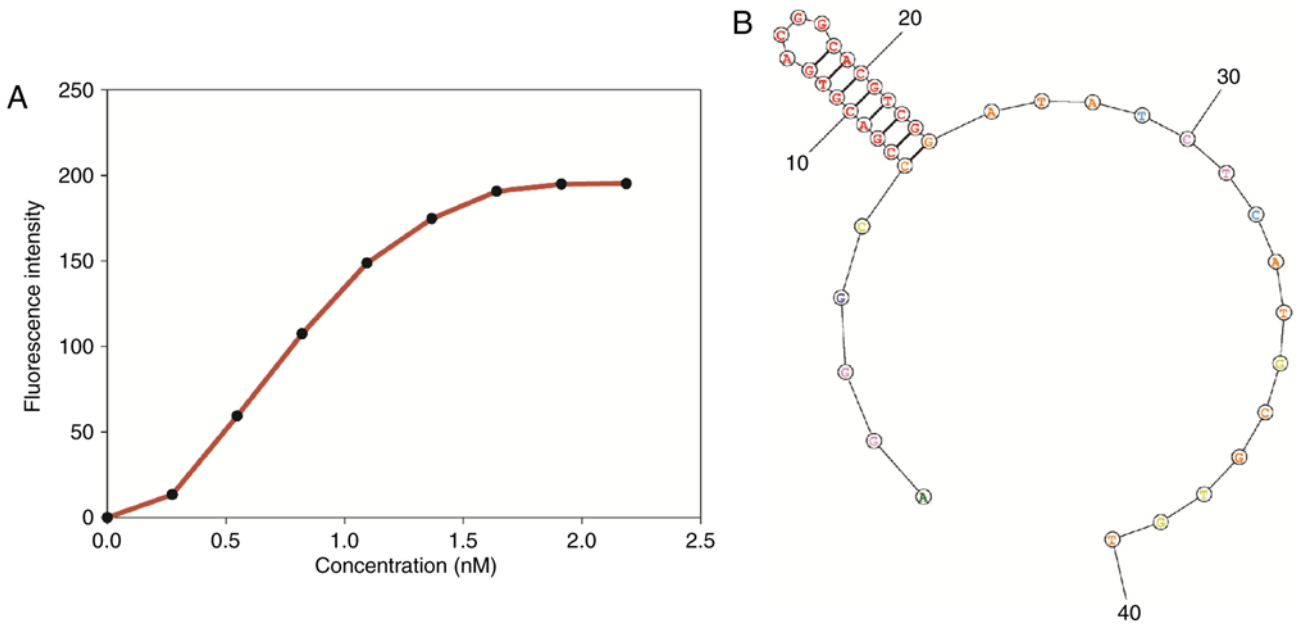

Figure 4. Flow cytometry was used to calculate the Kd of M17 for 293T-MMP14 cells. Kd, 4.98±1.26 nM. (A) Binding specificity of M17 to MMP14-positive cancer cell lines. (B) Secondary structure of M17 predicted by RNA structure. MMP14, matrix metalloproteinase 14; Kd, dissociation constant.

293T cells. A total of 36 h after transfection, western blotting revealed that MMP14 was overexpressed in 293T-MMP14 cells and expressed at an almost undetectable level in 293T-Plasmid cells (Fig. 1). This result indicated that two transfected cell lines were generated and there was a marked difference in the expression of MMP14 between them.

Screening results of DNA aptamers. In the cell-SELEX, 293T-MMP14 cells were used as positive screening cells. To reduce non-specific sequences, 293T-Plasmid cells were used as negative control cells. The enrichment effect of each selected round was monitored by flow cytometry. The fluorescence intensity of the cells indicated the binding affinity of the library. The fluorescence intensity of the 293T-MMP14 cells bound to the selected library increased with the number of selection rounds. However, no increase was observed in the 293T-Plasmid cells (Fig. 2A and B). The percentages of fluorescent-labeled cells at various stages of the process are presented in Table I. The results indicated that the ssDNA sequences that specifically bound to the target cells were gradually enriched. However, the degree of increase gradually decreased as the number of selection rounds increased. The screening process was completed after 12 rounds. The final library was amplified and cloned, then sequenced by Tsingke Biological Technology Co., Ltd. (Beijing, China).

Analysis and verification of ssDNA aptamers. After sequencing, 24 effective sequences were selected and synthesized by Sangon Biotech Co., Ltd. with a FAM label on the 5' end. Four representative sequences (M5, M12, M17 and M35) were selected by flow cytometry due to their high affinity for recognizing 293T-MMP14 cells. Among these, aptamer M17 demonstrated the highest affinity for 293T-MMP14 cells compared with 293T-Plasmid cells (Fig. 2C and D). When cells were incubated with the FAM-labeled aptamer M17, the

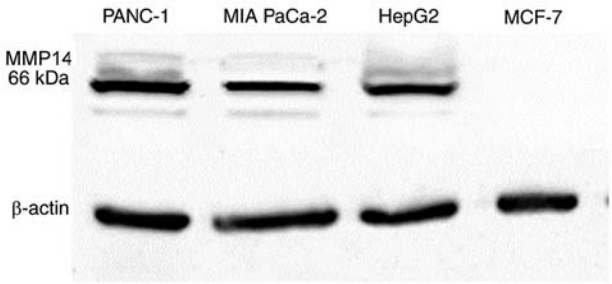

Figure 5. Expression levels of MMP14 protein in PANC-1, MIA PaCa-2, HepG2 and MCF-7 cells were analyzed by western blotting. β-actin was used as an internal control.

confocal imaging results demonstrated that the fluorescence signal was predominantly located around the 293T-MMP14 cells and not the 293T-Plasmid cells (Fig. 3). These results indicated that aptamer M17 discriminated 293T-MMP14 cells from control cells and that the binding site of aptamer M17 was located on the cell membrane. The Kd value of M17 to 293T-MMP14 cells was 4.98±1.26 nM (Fig. 4A), indicating that M17 could recognize 293T-MMP14 cells with high specificity and high affinity. The secondary structure of aptamer M17 (Fig. 4B) was predicted using RNAstructure (http://rna.urmc.rochester.edu/RNAstructureWeb/). The sequence of aptamer M17 is as follows: 5'-AGGGCCCGACGTGACGGCACGTCGGATATCTCATGCGTGT-3'.

To investigate the binding ability of aptamer M17 for MMP14-positive cell lines, PANC-1, MIA PaCa-2, HepG2 and MCF-7 were incubated with aptamer M17 labeled with FAM. The initial library labeled by FAM was used as a negative control. Western blotting revealed that PANC-1, MIA PaCa-2 and HepG2 cells highly expressed MMP14, while MCF-7 cells expressed an almost undetectable level of MMP14 (Fig. 5). As presented in Fig. 6, aptamer M17 markedly increased

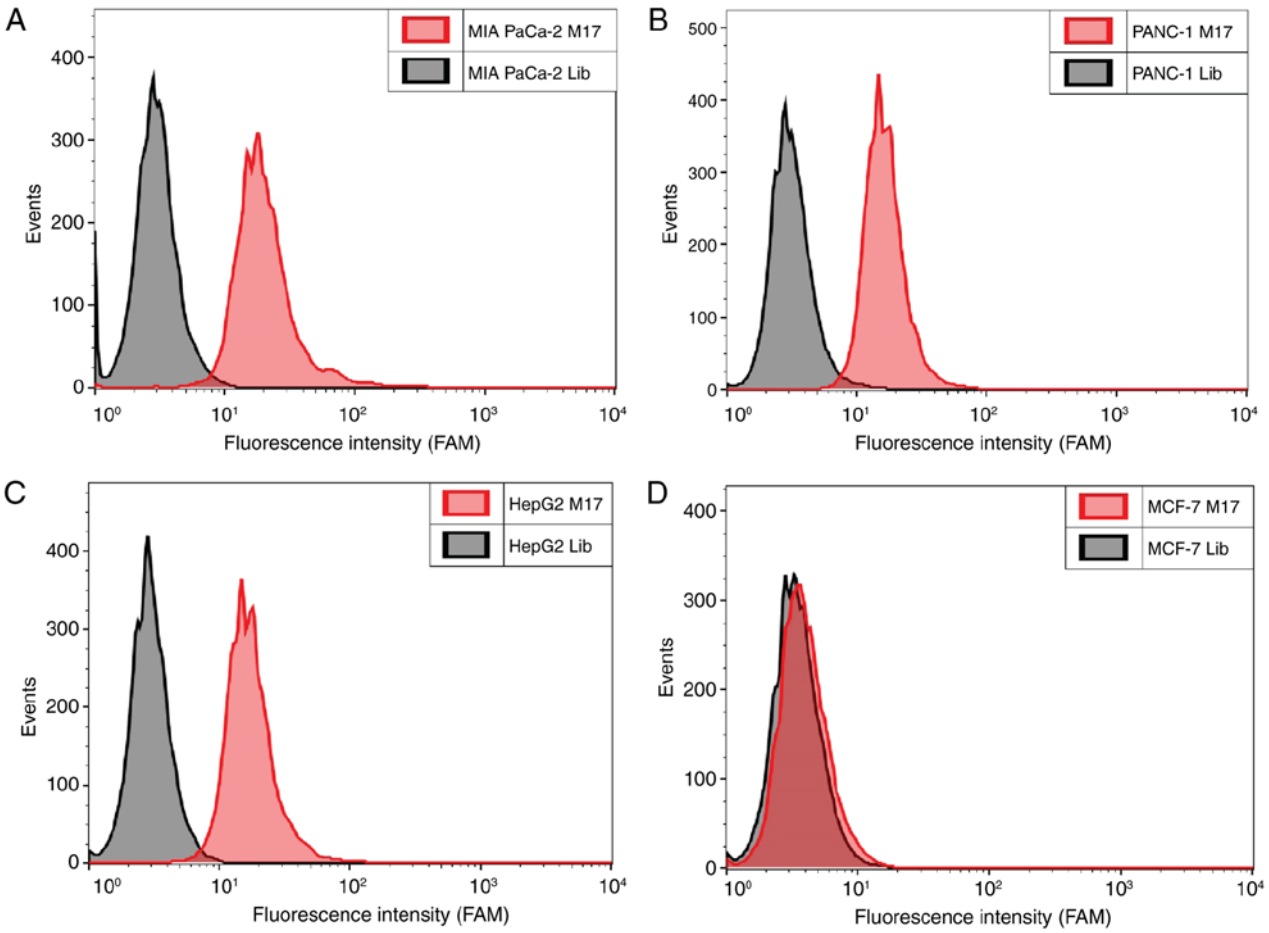

Figure 6. Binding specificity assays of FAM-M17 to different cancer cell lines, analyzed by flow cytometry. (A) MIA PaCa-2; (B) PANC-1; (C) HepG2, and (D) MCF-7. FAM, 5-carboxyfluorescein; Lib, initial library.

the fluorescence signal in pancreatic cancer (PANC-1, MIA PaCa-2) cells and hepatoblastoma (HepG2) cells, but not in breast cancer (MCF-7) cells. The selected initial library did not have this effect. These results indicate that the aptamer M17 could distinguish the MMP14-positive cancer cell lines from the MMP14-negative cell lines. However, it is not clear which part of MMP14 interacts with aptamer M17. Therefore, this was the main area of focus in the rest of the present study.

As presented in Fig. 7, The MIA PaCa-2 cells and PANC-1 cells were incubated with M17 labeled with Cy5 at 37˚C for 30 min. The results of confocal microscopy imaging revealed that M17 labeled by Cy5 specifically targeted the surface of the pancreatic cancer cell membrane.

In vivo fluorescence imaging for pancreatic tumor-bearing mice. To verify that the aptamer M17 had the ability to recognize MMP14 with high specificity *in vivo*, MIA PaCa-2-cell tumor-bearing nude mice were used. After the Cy5-labeled aptamer M17 was intravenously injected into the tumor-bearing nude mice for 3 min, a fluorescence signal was observed at the tumor site, which disappeared after 40 min. The Cy5-labeled initial library was also injected into the tumor-bearing nude mice, after which no fluorescence signal was evident at the tumor site at any observation time point (Fig. 8). These results indicate that the aptamer M17 could specifically recognize MIA PaCa-2 cells (MMP14-positive) *in vivo*, indicating that the aptamer M17 has a potential application for recognizing MMP14-positive cancer *in vivo*. The targeting residence time of aptamer M17 in the tumor-bearing nude mice was limited and completely disappeared after 40 min. The reason for this may be that the aptamer M17 was an unmodified aptamer. However, aptamer M17 successfully achieved targeted imaging of tumors. The next step may be to modify the aptamer to improve its nuclease resistance.

Synthesis of aptamer M17-conjugated magnetic nanoparticles and in vitro MRI. To verify the feasibility of SPIONs as MRI T2WI contrast agents, T2WI using different concentrations of SPIONs was performed using a 3.0T MRI scanner and the T2WI values were measured through the workstation. Fig. 9C presents T2WI images of a 3% agarose gel model with different concentrations of SPIONs. As the concentration of SPIONs increased, the brightness of the T2WI images decreased. Fig. 9A presents the correlation between SPIONs concentration and the T2WI value. The correlation coefficient (r=-0.738) indicated that the concentration of SPIONs was significantly negatively correlated with the T2WI value. This result indicates that SPIONs were effective T2WI darkening contrast agents.

To demonstrate the ability of M17-conjugated SPIONs (M17-SPIONs) to target pancreatic cancer cells for MRI *in vitro*, cells were incubated with M17-SPIONs probes at

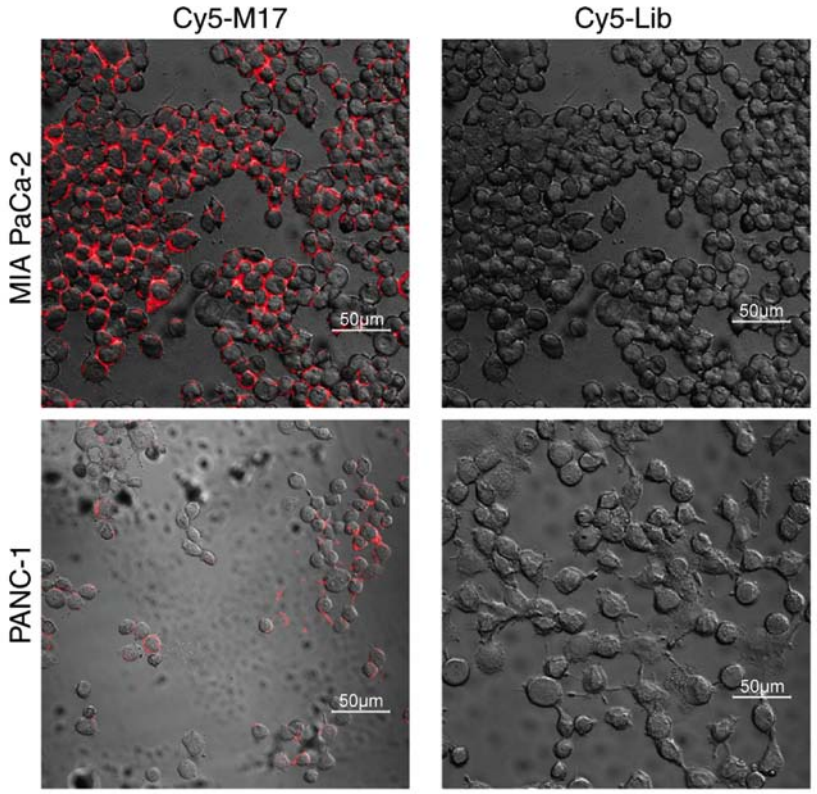

Figure 7. Binding specificity assays of the Cy5-labeled M17 to MIA PaCa2 cells and PANC-1 cells. Lib was used as a control. Scale bar, 50 μm. Lib, initial library.

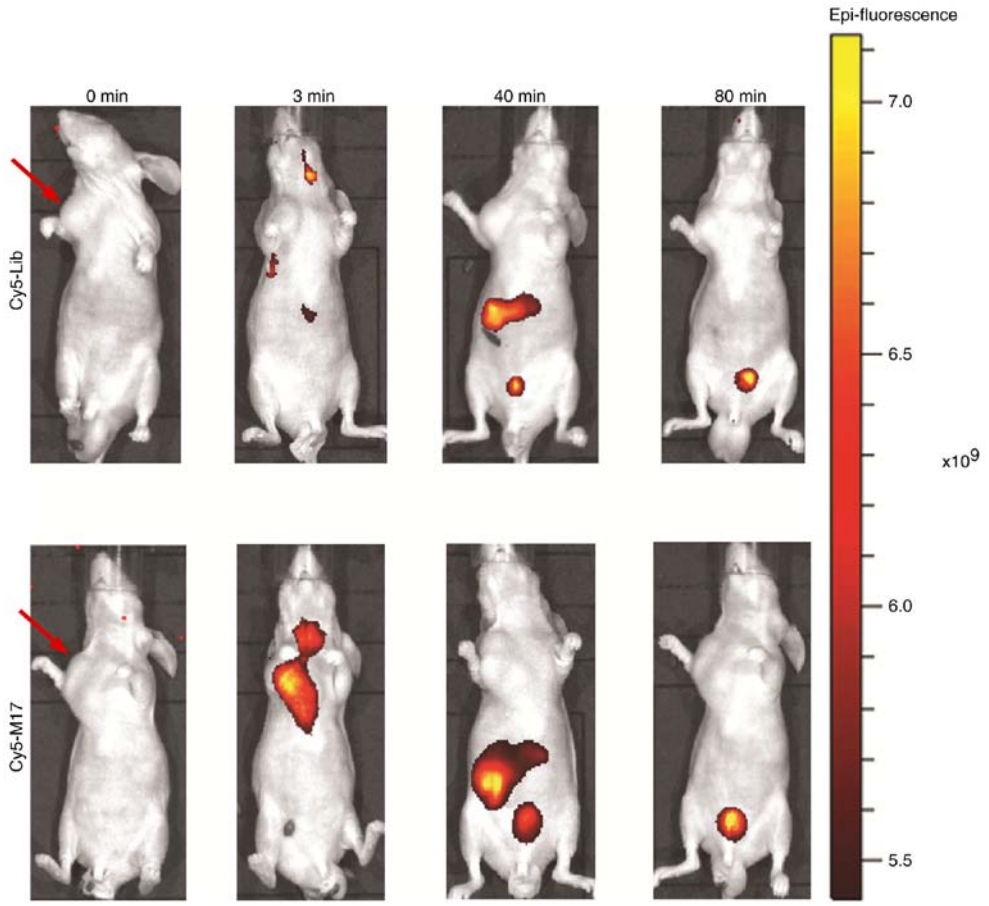

Figure 8. MIA PaCa-2 tumor-bearing nude mice were injected with Cy5-labeled library (upper panels) or Cy5-labeled aptamer M17 (lower panels) via the caudal vein, followed by fluorescence imaging at different time points. Tumor regions are shown by red arrows. Lib, initial library.

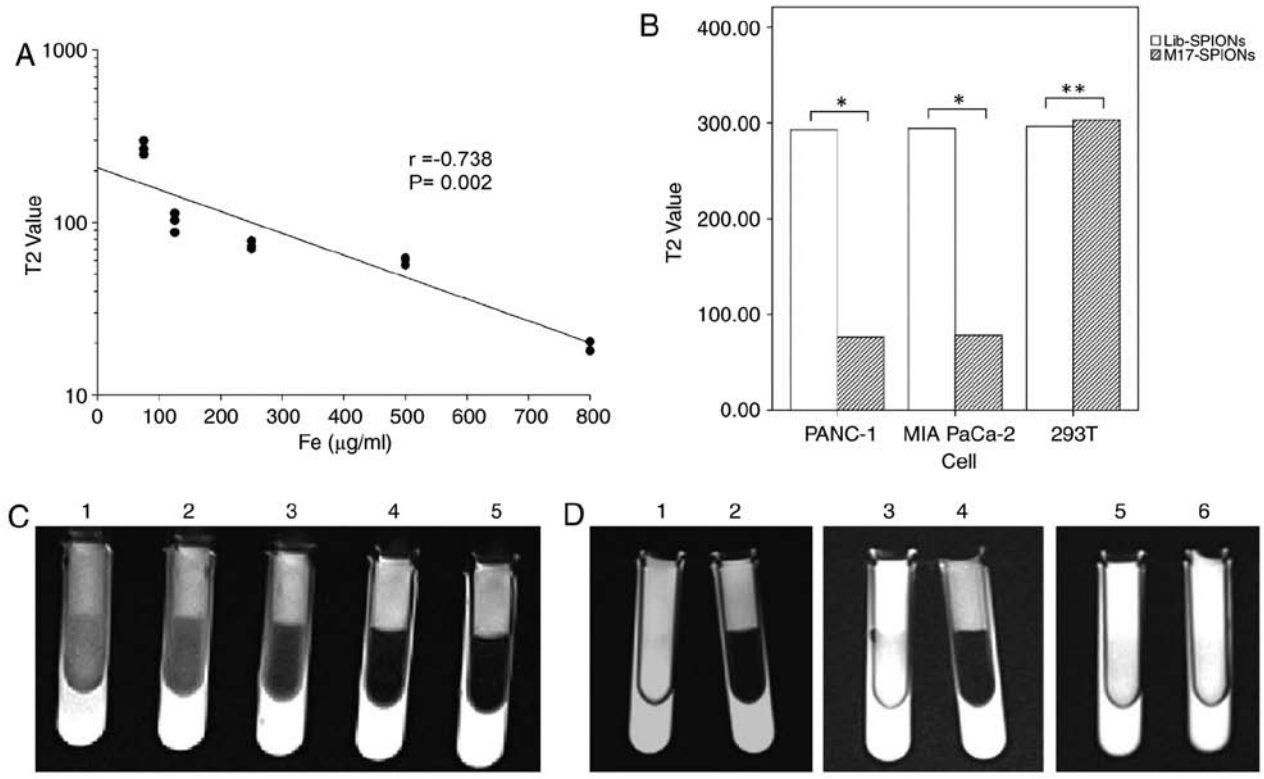

Figure 9. MRI measurements. (A) Correlation between T2 value and SPIONs concentration. The coefficient was r=-0.738 (P=0.002), as determined by Pearson's correlation analysis. (B) The T2 values of different cell groups incubated with M17-SPIONs or Lib-SPIONs. (C) T2WI images of different concentrations of SPIONs scanned by 3.0T MRI. The concentrations of SPIONs added to centrifugal tubes nos. 1-5 were 60, 120, 250, 500 and 800 μg/ml, respectively. (D) T2WI images of different cell lines incubated with M17-SPIONs or Lib-SPIONs scanned by 3.0T MRI. Centrifugal tubes 1 and 2 contained 293T cells, 3 and 4 contained Panc-1 cells, and 5 and 6 contained MIAPaCa-2 cells. Centrifugal tubes 1, 3 and 5 were incubated with SPIONs-M17, and 2, 4 and 6 were incubated with SPIONs-Lib. *P<0.01, **P>0.01. MRI, magnetic resonance imaging; SPION, superparamagnetic iron oxide nanoparticle; Lib, initial library; Fe, iron.

37˚C for 1 h. Subsequently, the cells were resuspended in 3% agarose gel. The T2WI images of different cells were scanned using a 3.0T MRI scanner. The Lib-SPIONs probes served as a negative control. Fig. 9D presents T2WI images of the different cell groups. The T2WI images of MIA PaCa-2 cells and PANC-1 cells incubated with M17-SPIONs were markedly darkened, while those of 293T cells were not. After incubation with Lib-SPIONs, the T2WI images did not darken for any cell group. Fig. 9B presents a histogram of T2WI values of the different cell groups incubated with two probes. These results indicate that M17-SPIONs effectively reduced T2WI values in MIA PaCa-2 and PANC-1 cells *in vitro*. The M17-SPIONs probe was demonstrated to be a potential MRI nanoprobe for pancreatic cancer. In the future, the conditions of probes (M17- SPIONs) applied in *in vivo* xenograft models should be optimized.

In conclusion, aptamer M17, which specifically recognized MMP14-positive cancer cells, was successfully obtained by Cell-SELEX after 12 rounds of screening. Aptamer M17 could bind to MMP14-transfected 293T cells with high specificity and high affinity, with a Kd value in the nanomolar range. Binding analysis revealed that aptamer M17 can recognize MMP14-positive cancer cells, including PANC-1, MIA PaCa-2 and HepG2 cells. Tumor imaging *in vivo* demonstrated that aptamer M17 has potential for targeted diagnosis and treatment of pancreatic cancer. In addition, aptamer M17-conjugated SPIONs (M17-SPIONs) demonstrated efficient targeted MRI of pancreatic cancer cells *in vitro*. In summary, DNA aptamer M17 is a promising molecular targeting agent and has potential application value in the targeted diagnosis and treatment of MMP14-positive cancer.

Acknowledgements

Not applicable.

Funding

The present study was supported by the National Natural Science Foundation of China (grant nos. NSFC 81220108011 and NSFC 81370039).

Availability of data and materials

Not applicable.

Authors' contributions

XH designed the experiment, wrote the manuscript, performed aptamer screening and managed the team. JZ cultured the cells, monitored the mice and test cells, and performed flow cytometry and fluorescence imaging. JR analyzed the data and reviewed the manuscript. DW constructed the tumor-bearing nude mice model and performed *in vivo* imaging of the mice. WZ performed magnetic resonance imaging of the cells. YH was responsible for assessing the feasibility of the study

design, guiding the experimental process and the assessment of data accuracy. In addition, YH agreed to be accountable for all aspects of the work in ensuring that questions related to the accuracy or integrity of any part of the work are appropriately investigated and resolved and gave final approval of the manuscript version to be published. All authors read and approved the final manuscript.

Ethics approval and consent to participate

This study was approved by the Ethics Committee of the Experimental Animal Center of the Fourth Military Medical University (Xi'an, China). The relevant proofs are filed at the Animal Experimental Center.

Patient consent for publication

Not applicable.

Competing interests

The authors declare that they have no competing interests.

References

1. Brinckerhoff CE and Matrisian LM: Matrix metalloproteinases: A tail of a frog that became a prince. Nat Rev Mol Cell Biol 3: 207-214, 2002.
2. Suzuki A, Lu J, Kusakai G, Kishimoto A, Ogura T and Esumi H: ARK5 is a tumor invasion-associated factor downstream of Akt signaling. Mol Cell Biol 24: 3526-3535, 2004.
3. Seiki M: Membrane-type 1 matrix metalloproteinase: A key enzyme for tumor invasion. Cancer Lett 194: 1-11, 2003.
4. Galvez BG, Matias-Roman S, Albar JP, Sanchez-Madrid F and Arroyo AG: Membrane type 1-matrix metalloproteinase is activated during migration of human endothelial cells and modulates endothelial motility and matrix remodeling. J Biol Chem 276: 37491-37500, 2001.
5. Arroyo AG, Genis L, Gonzalo P, Matias-Roman S, Pollan A and Galvez BG: Matrix metalloproteinases: New routes to the use of MT1-MMP as a therapeutic target in angiogenesis-related disease. Curr Pharm Des 13: 1787-1802, 2007.
6. Wickramasinghe RD, Ko Ferrigno P and Roghi C: Peptide aptamers as new tools to modulate clathrin-mediated internalisation-inhibition of MT1-MMP internalisation. BMC Cell Biol 11: 58, 2010.
7. Ottaviano AJ, Sun L, Ananthanarayanan V and Munshi HG: Extracellular matrix-mediated membrane-type 1 matrix metalloproteinase expression in pancreatic ductal cells is regulated by transforming growth factor-beta1. Cancer Res 66: 7032-7040, 2006.
8. Imamura T, Ohshio G, Mise M, Harada T, Suwa H, Okada N, Wang Z, Yoshitomi S, Tanaka T, Sato H, *et al*: Expression of membrane-type matrix metalloproteinase-1 in human pancreatic adenocarcinomas. J Cancer Res Clin Oncol 124: 65-72, 1998.
9. Chen TY, Li YC, Liu YF, Tsai CM, Hsieh YH, Lin CW, Yang SF and Weng CJ: Role of MMP14 gene polymorphisms in susceptibility and pathological development to hepatocellular carcinoma. Ann Surg Oncol 18: 2348-2356, 2011.
10. Sato H, Takino T, Okada Y, Cao J, Shinagawa A, Yamamoto E and Seiki M: A matrix metalloproteinase expressed on the surface of invasive tumour cells. Nature 370: 61-65, 1994.
11. Tokuraku M, Sato H, Murakami S, Okada Y, Watanabe Y and Seiki M: Activation of the precursor of gelatinase A/72 kDa type IV collagenase/MMP-2 in lung carcinomas correlates with the expression of membrane-type matrix metalloproteinase (MT-MMP) and with lymph node metastasis. Int J Cancer 64: 355-359, 1995.
12. Polette M, Nawrocki B, Gilles C, Sato H, Seiki M, Tournier JM and Birembaut P: MT-MMP expression and localisation in human lung and breast cancers. Virchows Arch 428: 29-35, 1996.
13. Nawrocki B, Polette M, Marchand V, Monteau M, Gillery P, Tournier JM and Birembaut P: Expression of matrix metalloproteinases and their inhibitors in human bronchopulmonary carcinomas: Quantificative and morphological analyses. Int J Cancer 72: 556-564, 1997.
14. Mori M, Mimori K, Shiraishi T, Fujie T, Baba K, Kusumoto H, Haraguchi M, Ueo H and Akiyoshi T: Analysis of MT1-MMP and MMP2 expression in human gastric cancers. Int J Cancer 74: 316-321, 1997.
15. Nomura H, Sato H, Seiki M, Mai M and Okada Y: Expression of membrane-type matrix metalloproteinase in human gastric carcinomas. Cancer Res 55: 3263-3266, 1995.
16. Bando E, Yonemura Y, Endou Y, Sasaki T, Taniguchi K, Fujita H, Fushida S, Fujimura T, Nishimura G, Miwa K and Seiki M: Immunohistochemical study of MT-MMP tissue status in gastric carcinoma and correlation with survival analyzed by univariate and multivariate analysis. Oncol Rep 5: 1483-1488, 1998.
17. Ohtani H, Motohashi H, Sato H, Seiki M and Nagura H: Dual over-expression pattern of membrane-type metalloproteinase-1 in cancer and stromal cells in human gastrointestinal carcinoma revealed by in situ hybridization and immunoelectron microscopy. Int J Cancer 68: 565-570, 1996.
18. Ueno H, Nakamura H, Inoue M, Imai K, Noguchi M, Sato H, Seiki M and Okada Y: Expression and tissue localization of membrane-types 1, 2, and 3 matrix metalloproteinases in human invasive breast carcinomas. Cancer Res 57: 2055-2060, 1997.
19. Jones JL, Glynn P and Walker RA: Expression of MMP-2 and MMP-9, their inhibitors, and the activator MT1-MMP in primary breast carcinomas. J Pathol 189: 161-168, 1999.
20. Wang L, Yuan J, Tu Y, Mao X, He S, Fu G, Zong J and Zhang Y: Co-expression of MMP-14 and MMP-19 predicts poor survival in human glioma. Clin Transl Oncol 15: 139-145, 2013.
21. Gilles C, Polette M, Piette J, Munaut C, Thompson EW, Birembaut P and Foidart JM: High level of MT-MMP expression is associated with invasiveness of cervical cancer cells. Int J Cancer 65: 209-213, 1996.
22. Zhang ZH, Wen DD, Fu X, Zhong JM, Lu JT, Huang XF, Ren J, Yang Y and Huan Y: Study on the expression and clinical significance of survivin and MMP14 in pancreatic cancer. Progress in Modern Biomed 15: 3022-3027, 2015 (In Chinese).
23. Shimizu Y, Temma T, Sano K, Ono M and Saji H: Development of membrane type-1 matrix metalloproteinase-specific activatable fluorescent probe for malignant tumor detection. Cancer Sci 102: 1897-1903, 2011.
24. Devy L, Huang L, Naa L, Yanamandra N, Pieters H, Frans N, Chang E, Tao Q, Vanhove M, Lejeune A, *et al*: Selective inhibition of matrix metalloproteinase-14 blocks tumor growth, invasion, and angiogenesis. Cancer Res 69: 1517-1526, 2009.
25. Ingvarsen S, Porse A, Erpicum C, Maertens L, Jurgensen HJ, Madsen DH, Melander MC, Gardsvoll H, Hoyer-Hansen G, Noel A, *et al*: Targeting a single function of the multifunctional matrix metalloprotease MT1-MMP: Impact on lymphangiogenesis. J Biol Chem 288: 10195-10204, 2013.
26. Haage A, Nam DH, Ge X, Schneider IC: Matrix metalloproteinase-14 is a mechanically regulated activator of secreted MMPs and invasion. Biochem Biophys Res Commun 450: 213-218, 2014.
27. Udi Y, Grossman M, Solomonov I, Dym O, Rozenberg H, Moreno V, Cuniasse P, Dive V, Arroyo AG and Sagi I: Inhibition mechanism of membrane metalloprotease by an exosite-swiveling conformational antibody. Structure 23: 104-115, 2015.
28. Chung E, Ochs CJ, Wang Y, Lei L, Qin Q, Smith AM, Alex S, Kamm RD, Qi YX, Lu S and Wang YP: Activatable and Cell-Penetrable Multiplex FRET Nanosensor for Profiling MT1-MMP Activity in Single Cancer Cells. Nano Lett 15: 5025-5032, 2015.
29. Sefah K, Shangguan D, Xiong X, O'Donoghue MB and Tan W: Development of DNA aptamers using Cell-SELEX. Nat Protoc 5: 1169-1185, 2010.
30. Ellington AD and Szostak JW: In vitro selection of RNA molecules that bind specific ligands. Nature 346: 818-822, 1990.
31. Tuerk C and Gold L: Systematic evolution of ligands by exponential enrichment: RNA ligands to bacteriophage T4 DNA polymerase. Science 249: 505-510, 1990.
32. Shangguan D, Li Y, Tang Z, Cao ZC, Chen HW, Mallikaratchy P, Sefah K, Yang CJ and Tan W: Aptamers evolved from live cells as effective molecular probes for cancer study. Proc Natl Acad Sci USA 103: 11838-11843, 2006.
33. Liu J, You M, Pu Y, Liu H, Ye M and Tan W: Recent developments in protein and cell-targeted aptamer selection and applications. Curr Med Chem 18: 4117-4125, 2011.

34. Xing H, Wong NY, Xiang Y and Lu Y: DNA aptamer functionalized nanomaterials for intracellular analysis, cancer cell imaging and drug delivery. Curr Opin Chem Biol 16: 429-435, 2012.
35. Hwang DW, Ko HY, Lee JH, Kang H, Ryu SH, Song IC, Lee DS and Kim S: A nucleolin-targeted multimodal nanoparticle imaging probe for tracking cancer cells using an aptamer. J Nucl Med 51: 98-105, 2010.
36. Mosafer J, Abnous K, Tafaghodi M, Mokhtarzadeh A and Ramezani M: In vitro and in vivo evaluation of anti-nucleolin-targeted magnetic PLGA nanoparticles loaded with doxorubicin as a theranostic agent for enhanced targeted cancer imaging and therapy. Eur J Pharm Biopharm 113: 60-74, 2017.
37. You XG, Tu R, Peng ML, Bai YJ, Tan M, Li HJ, Guan J and Wen LJ: Molecular magnetic resonance probe targeting VEGF165: Preparation and in vitro and in vivo evaluation. Contrast Media Mol Imaging 9: 349-354, 2014.
38. Pu Y, Liu Z, Lu Y, Yuan P, Liu J, Yu B, Wang G, Yang CJ, Liu H and Tan W: Using DNA aptamer probe for immunostaining of cancer frozen tissues. Anal Chem 87: 1919-1924, 2015.
39. Pilapong C, Sitthichai S, Thongtem S and Thongtem T: Smart magnetic nanoparticle-aptamer probe for targeted imaging and treatment of hepatocellular carcinoma. Int J Pharm 473: 469-474, 2014.
40. Li CH, Kuo TR, Su HJ, Lai WY, Yang PC, Chen JS, Wang DY, Wu YC and Chen CC: Fluorescence-guided probes of aptamer-targeted gold nanoparticles with computed tomography imaging accesses for in vivo tumor resection. Sci Rep 5: 15675, 2015.